

---

# IPGO: Indirect Prompt Gradient Optimization on Text-to-Image Generative Models with High Data Efficiency

---

Jianping Ye<sup>1</sup> Michel Wedel<sup>1</sup> Kunpeng Zhang<sup>1</sup>

<sup>1</sup>The University of Maryland, College Park, MD 20742, USA  
 {jpye00,mwedel,kpzhang}@umd.edu

## Abstract

Text-to-Image Diffusion models excel at generating images from text prompts but often lack optimal alignment with content semantics, aesthetics, and human preferences. To address these issues, in this study we introduce a novel framework, Indirect Prompt Gradient Optimization (IPGO), for prompt-level fine-tuning. IPGO enhances prompt embeddings by injecting continuously differentiable tokens at the beginning and end of the prompt embeddings, while exploiting low-rank benefits and flexibility from rotations. It allows for gradient-based optimization of injected tokens while enforcing value, orthonormality, and conformity constraints, facilitating continuous updates and empowering computational efficiency. To evaluate the performance of IPGO, we conduct prompt-wise and prompt-batch training with three reward models targeting image aesthetics, image-text alignment, and human preferences under three datasets of different complexity. The results show that IPGO consistently matches or outperforms cutting-edge benchmarks, including stable diffusion v1.5 with raw prompts, training-based approaches (DRaFT and DDPO), and training-free methods (DPO-Diffusion, Promptist, and ChatGPT-4o). Furthermore, we demonstrate IPGO’s effectiveness in enhancing image generation quality while requiring minimal training data and limited computational resources<sup>1</sup>.

## 1. Introduction

Text-to-Image (T2I) Diffusion models have become state-of-the-art pipelines for image generation (Zhang et al., 2023; Liu et al., 2024) due to their powerful ability to translate text prompts into images. Users can input any written text

<sup>1</sup>Code is available for reproducibility: <https://github.com/Demos750/IPGO>

into the model, which then generates the corresponding image. However, not all generated images meet high-quality standards with reference to specific downstream objectives (Liu et al., 2024). Often, aligning images with human preferences is desired, necessitating further image optimization. Consequently, users have to experiment with text prompts to produce images that align better with measures of aesthetics, human preferences, and other criteria (Wang et al., 2022). Unfortunately, many downstream applications lack clear and instructive guidelines for prompt design (Liu & Chilton, 2022), making systematic manual prompt engineering challenging or even infeasible. To avoid such laborious prompt engineering, several approaches have been proposed, ranging from automatic prompt optimization to generative model fine-tuning (Black et al., 2023; Hao et al., 2024; Fan et al., 2024; Prabhudesai et al., 2023; Liu et al., 2024). However, many of these methods either require data-intensive training techniques such as Supervised Fine-Tuning (SFT) and Reinforcement Learning (RL), or require uniquely modifying the generative model itself for each downstream task, thereby hampering practical applications. Therefore, there remains a keen interest in developing resource-efficient, systematic frameworks for image optimization in alignment tasks.

In this paper, we propose a novel prompt optimization framework, named Indirect Prompt Gradient Optimization (IPGO), which can be applied to both individual images and image batches. Instead of directly optimizing the input prompt, we inject continuously differentiable tokens at the beginning and end of the text feature space - where text embeddings encoded by the text encoder dwell - employ constrained gradient-based optimization on these injected tokens. This approach facilitates continuous gradient updates and circumvents the difficulty associated with the discrete nature of actual prompt inputs. To evaluate our IPGO method, we conduct experiments using the Stable Diffusion Model V1.5 (Rombach et al., 2022) on a single GPU. We assess performance based on three target reward models: image aesthetics (Schuhmann, 2024), image-text alignment (Radford et al., 2021), human preference scores (Wu et al., 2023). Overall, our results show that IPGO is effective for prompt optimization while requiring minimal training data

and limited computational resources. Our contributions are as follows:

- (1) We introduce a novel gradient-based prompt optimization framework for text-to-image diffusion models that optimizes continuous tokens injected at the beginning and end of the prompt embeddings.
- (2) IPGO is effective in handling prompt batches for training, achieving more desirable reward properties because the learned inserted tokens are shared across all prompts within a batch.
- (3) Extensive experiments are conducted on different datasets to validate IPGO’s superiority across various reward functions. The results show that with the same number of generations from the diffusion model and identical resource allocation (batch size and number of GPUs), IPGO outperforms several SOTA gradient-based methods in most cases.

## 2. Related Work

**Text-to-Image Models** Recent advancements in text-to-image generation have been extensively reviewed by several researchers, including (Frolov et al., 2021; Żelaszczyk & Mańdziuk, 2024; Zhang et al., 2023). Text-to-Image generative models typically use an encoder/decoder architecture. Żelaszczyk and Mańdziuk (Żelaszczyk & Mańdziuk, 2024) categorize these models based on their underlying frameworks, which include variational autoencoders (VAEs) (Kingma, 2013), generative adversarial networks (GANs) (Goodfellow et al., 2014), or diffusion models (DMs) (Sohl-Dickstein et al., 2015). According to Zhang and coauthors (Zhang et al., 2023), diffusion models have emerged as the most prominent and effective approach for text-to-image generation.

**Diffusion Probabilistic Models** Foundational work in Text-to-Image generation using diffusion models includes score-based generative models (Song & Ermon, 2019) and diffusion-probabilistic models (Sohl-Dickstein et al., 2015). A landmark development in this field was the introduction of the denoising diffusion probabilistic model (DDPM) (Ho et al., 2020). Subsequent diffusion models, such as GLIDE (Nichol et al., 2021) and Imagen (Saharia et al., 2022) operate the diffusion process directly in pixel space. In contrast, methods like Stable Diffusion (Rombach et al., 2022) and DALL-E (Ramesh et al., 2022) apply the diffusion process in a low-dimensional space, where images are projected using pre-trained autoencoders. Notably, Stable Diffusion has demonstrated superior image quality and efficiency compared to other models (Zhang et al., 2023). Since its inception, several extensions and improvements to the Stable Diffusion framework have been proposed (e.g., Podell et al.,

2023; Peebles & Xie, 2023; Esser et al., 2024).

A significant challenge with diffusion models is that the images they generate from text prompts often fail to align with human preferences. Thus, a growing body of research has emerged, focusing on controlling image generation by optimizing pre-trained diffusion models to better reflect human-preferred properties (Liu et al., 2024). This alignment can be achieved either during training of the model or through training-free methods.

**Training-based alignment (Liu et al., 2024)** uses supervised fine-tuning (SFT) of the diffusion model combined with reinforcement learning from human feedback (RLHF) to align the model with human preferences. This approach uses a reward model as a proxy for human preferences. Models in this category, such as ReFL (Xu et al., 2024), DDPO (Black et al., 2023), AlignProp (Prabhudesai et al., 2023), DRaFT (Clark et al., 2023), DPOK (Fan et al., 2024), DPO-Diffusion (Wang et al., 2024) and ReNeg (Li et al., 2024), rely on gradient-based fine-tuning of the diffusion model. Alternatively, models can be directly optimized on preference data using methods like Direct Preference Optimization (DPO), as seen in Diffusion-DPO (Wallace et al., 2024), D3PO (Yang et al., 2024a), and SPO (Liang et al., 2024).

**Training-free alignment (Liu et al., 2024)** aligns diffusion models with human preferences without the need for fine-tuning. The primary approach employed is prompt optimization, which can be conducted manually by users or through systematic approaches that have been proposed (Oppenlaender, 2023). For instance, RePrompt (Wang et al., 2023) is a prompt editing approach based on a curated rubric of text features. Mathematical approaches to prompt optimization include Promptist (Hao et al., 2024), which uses supervised fine-tuning and reinforcement learning on large language models (LLMs) to refine prompts, and OPT2I (Mañas et al., 2024), which uses an LLM to iteratively adapt prompts. Additionally, DPO-Diffusion (Wang et al., 2024) involves a discrete optimization within a compact subspace of the most relevant prompt words in the negative prompt space. PEZ (Wen et al., 2024) applies gradient-based discrete prompt optimization by applying the gradient of prompt embeddings, projected to their nearest neighbor in the continuous embedding. ReNeg (Li et al., 2024) directly learns negative prompt embeddings using gradients derived from reward models.

Other training-free strategies focus on optimizing the initial noise distribution for the reverse diffusion process to align with certain rewards (Samuel et al., 2024; Kim et al., 2024), or involve manipulating self- and cross-attention mechanisms to improve alignment (Chefer et al., 2023; Wu et al., 2024; Yang et al., 2024b; Zheng et al., 2023). These

approaches collectively contribute to aligning diffusion models with human preferences without the need for extensive retraining.

### 3. Preliminaries

**Diffusion Models** In essence, diffusion models are probabilistic models that construct an image conditioned on a text prompt by denoising the image from a pure Gaussian noise followed by sequential noise removal with an (UNet-based) error model  $\epsilon_\theta$  (Rombach et al., 2022) which predicts the noise to reduce at each noisy image  $x_t$  and is trained via maximizing a variational lower bound equivalent to (Ho et al., 2020):

$$\mathcal{L}(\theta) = \mathbb{E}_{t \sim U(0, T), x_0 \sim p_{\text{data}}, \epsilon \sim \mathcal{N}(0, I)} [\|\epsilon - \epsilon_\theta(x_t, t)\|^2].$$

Text-to-image diffusion models can either be trained using a guidance function (Dhariwal & Nichol, 2021) or with classifier-free guidance (Ho & Salimans, 2022).

**Reward Models** Typically, a generated image is evaluated using a pre-trained reward model, denoted as  $\mathcal{R}$ . The reward model assesses how well an image produced by a diffusion model aligns with human preferences. For each image  $x$  generated by the diffusion model in response to a prompt  $C$ , the reward model assigns a reward  $\mathcal{R}(x, C)$ , which serves as a proxy for human evaluation of the prompt-image pair. The reward  $\mathcal{R}(x, C)$  is then used to guide the diffusion model towards generating more preferred images through optimization. The reward model is initialized using a pre-trained LLM, and is fine-tuned on human-collected preference data by replacing its final layer with a regression layer. Among the widely used reward models are the LAION aesthetic predictor V2 (Schuhmann, 2024), the CLIP loss derived from the multimodal CLIP model (Radford et al., 2021), and the human preference score v2 (Wu et al., 2023). These models play a critical role in aligning the outputs of diffusion models with human preferences.

### 4. Methods

In this section, we formally introduce our method IPGO for image optimization with diffusion models. The general problem is formulated as follows. Let  $C$  denote the given prompt(s),  $\mathcal{R}$  be the trained external reward model, and  $p$  be the pre-trained diffusion model. We aim to optimize  $C$  such that the expected rewards of the corresponding images generated by the diffusion model  $g$  are maximized. This can be expressed as maximizing the following objective function  $\mathcal{L}$ :

$$\mathcal{L} = \mathbb{E}_{C \sim p(C), x \sim p(x|C)} \mathcal{R}(x, C), \quad (1)$$

where  $p(C)$  is the prompt distribution, and  $p(x|C)$  is the image distribution conditioned on the prompt. In the following

sections, we first present the motivation behind our approach and outline the overall framework. Figure 1 illustrates the IPGO methodology.

#### 4.1. IPGO

Optimizing prompts  $C$  directly is challenging due to the discrete nature of tokens, which prevents access to gradients with respect to the reward model. To address this, our key insight is to optimize the prompt indirectly by optimizing its projections onto the latent space of the text encoder. Specifically, in diffusion models, the text prompts  $C$  are first transformed into text embeddings using a text encoder  $f$  (typically a transformer, such as the text transformer in Stable Diffusion v1.5). These embeddings, denoted as  $f(C) \in \mathbb{R}^{d \times S}$ , where  $d$  is the embedding dimension and  $S$  is the length of the token sequence, are then fed into the diffusion model  $g$  to generate the image. Importantly, embeddings  $E$  are not inherently discrete, allowing us to optimize the actual inputs to  $g$ .

**Constrained Prefix-Suffix Tuning** Inspired by Prefix-Tuning (Li & Liang, 2021) in Large Language Models, we propose a method for diffusion models that involves adding extra continuously differentiable tokens before and after the original text embeddings. Additionally, to further enhance flexibility, we add free tokens at the end of each text embedding sequence. Denote the prefix tokens as  $V_{pre} \in \mathbb{R}^{d \times M_{pre}}$  and the suffix tokens as  $V_{suf} \in \mathbb{R}^{d \times M_{suf}}$ , where  $M$ 's are the number of tokens inserted. Given a pre-trained text encoder  $f$  and a user prompt input  $C$ , the updated text embedding sequence for the diffusion model is constructed as follows:

$$T = \text{concat}(V_{pre}, f(C), V_{suf}), \quad (2)$$

where  $\text{concat}(\cdot)$  indicates concatenation in the dimension representing the sequence length. To enhance the optimization flexibility, rather than directly optimizing  $V_{pre}$  and  $V_{suf}$ , we model the extra tokens as linear combinations of a set of learnable embeddings, followed by a specific rotation operation controlled by learnable angles. Specifically, let  $E \in \mathbb{R}^{d \times N}$  denote the learnable embeddings, where  $N \ll d$  is the number of learnable embeddings. Let  $Z \in \mathbb{R}^{N \times M}$  represent the affine transformation coefficients, and  $\theta \in (-\pi, \pi]^2$  denote the learnable angles. The rotation operation is comprised of two coordinate-wise rotations, achieved via the elementary rotation matrix:

$$R_{e, \alpha} = \begin{bmatrix} \cos \alpha & -\sin \alpha \\ \sin \alpha & \cos \alpha \end{bmatrix}. \quad (3)$$

Next, we define two rotations via coordinate-wise rotation matrices:  $R_{1, \theta_1} \in \mathbb{R}^{d \times d}$  and  $R_{2, \theta_2} \in \mathbb{R}^{d \times d}$ :

$$R_{1, \theta_1} = I_{d/2} \otimes R_{e, \theta_1} \quad (4)$$

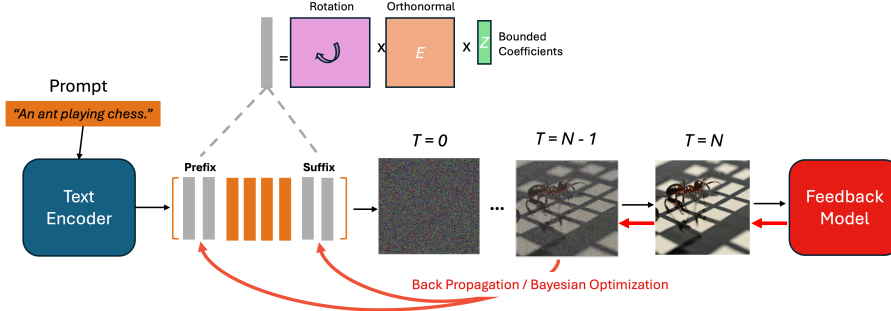


Figure 1. IPGO inserts trainable tokens to the prompt in the CLIP text encoder space and then sends back feedback signals through either backpropagation (if the feedback model is differentiable) or a black-box optimization scheme such as Bayesian Optimization (if the feedback model is non-differentiable). We truncate the differentiation at the last sampling step.

$$R_{2,\theta_2} = \begin{bmatrix} R_{e,\theta_2,(2)} & & \\ & I_{d/2-1} \otimes R_{e,\theta_2} & \\ & & R_{e,\theta_2,(1)} \end{bmatrix}, \quad (5)$$

where  $\otimes$  is the tensor product,  $I$  is the identity matrix,  $R_{e,\theta_2,(i)}$  is the  $i^{\text{th}}$  row of  $R_{e,\theta_2}$ . Both  $R_{1,\theta_1}$  and  $R_{2,\theta_2}$  rotate adjacent pairs of coordinates. However,  $R_1$  rotates  $(2k-1, 2k)$  pairs, while  $R_2$  rotates  $(2k, 2k+1)$  pairs of coordinates, where  $k = 1, \dots, d/2$ . Note that the  $(d+1)^{\text{th}}$  entry is the  $1^{\text{st}}$  entry. Finally, the prefix- and suffix-tokens can be expressed by:

$$V_{pre} = R_{2,\theta_2^{pre}} R_{1,\theta_1^{pre}} E_{pre} Z_{pre}, \quad (6)$$

$$V_{suf} = R_{2,\theta_2^{suf}} R_{1,\theta_1^{suf}} E_{suf} Z_{suf}. \quad (7)$$

The intuition behind this formulation is that the embedding sets  $E$  define a subspace in the text embedding space, and the rotations allow for non-linearity. As a result, this parameterization enhances the expressiveness compared to the original embedding. However, to preserve the structural integrity of the text embeddings generated by the text encoder  $f$ , additional constraints are imposed to ensure successful training. To mitigate excessive perturbations to the embedding structures, we first add an **Orthonormality Constraint** to the embedding sets  $E$ , i.e.,

$$E_{pre} E_{pre}^T = I_{N_{pre}}, \quad E_{suf} E_{suf}^T = I_{N_{suf}}. \quad (8)$$

To further mitigate unwanted fluctuations, we introduce a **Value Constraint**, which restricts the values of the affine transformation coefficients  $Z$  to the range  $[-1, 1]$ . By enforcing orthonormality with constrained coefficients, we reduce the likelihood of exploring extremely unlikely text embeddings relative to the original distribution implied by  $f(C)$ . In addition, we add a **Conformity Constraint** to ensure that the embeddings of the inserted tokens align closely with those of the original prompt, promoting consistency and coherence in the generated outputs:

$$\frac{1}{J} \sum_{j=1}^J T_j = \frac{1}{K} \sum_{k=1}^K f(C)_k, \quad (9)$$

where the subscripts  $j$  and  $k$  represent the  $j^{\text{th}}$ ,  $k^{\text{th}}$  columns of the corresponding embedding matrices.

In summary, we have the following optimization objective:

$$\begin{aligned} \max_{\Theta} \quad & \mathbb{E}_{C \sim p(C), x \sim p(x|C)} \mathcal{R}(x, C) \\ \text{s.t.} \quad & (8), (9), Z_{ij} \in [-1, 1], \\ & \theta^{pre} \in [-\pi, \pi]^2, \theta^{suf} \in [-\pi, \pi]^2, \end{aligned} \quad (10)$$

where  $\Theta = \{E_{pre}, E_{suf}, Z_{pre}, Z_{suf}, \theta^{pre}, \theta^{suf}\}$ .

**Remarks:** Notice that our formulation for  $V$ 's is related to LoRA (Hu et al., 2021) and RoPE (Su et al., 2024), as both of these parameterizations exploit a low-rank structure and rotations. But our formulation for the prompt optimization context has much stronger constraints and operates entirely on the prompt-level instead of during model fine-tuning. Our rotation operations, unlike RoPE, are not designed to encode positions, but to add non-linearity and enlarge the search space by including trainable angle parameters.

**Backprop Truncation** We adopt the same backprop truncation method as described in DRaFT (Clark et al., 2023) to reduce the memory cost during training. Specifically, we set  $K = 1$ , meaning that backprop terminates at the final sampling step.

**Gradient Clipping** Following DRaFT, we apply gradient clipping across all our experiments, selecting a gradient clipping norm of  $c = 1.0$ .

## 5. Experiments

In this section, we first introduce the experiment settings (see Sec.5.1) and the benchmarks (see Sec.5.2). Evaluations and comparisons with baselines for individual prompt optimization are presented in Sec.5.3. Sec.5.4 presents the results of prompt-batch training. A detailed ablation study and analysis are provided in Sec.5.5.



## 5.1. Experiment Settings

**Datasets.** We evaluate our method using three datasets: the COCO image captions (Lin et al., 2014), Diffusiondb (Wang et al., 2022) and Pick-a-Pic datasets (Kirstain et al., 2023). These datasets represent a diverse range of prompts and images with varying levels of complexity. To assess the performance of IPGO across different categories of image captions, we conduct separate evaluations for COCO images in the categories of Persons, Rooms, Vehicles, Natural Scenes, and Buildings. For each category, we randomly select 60 captions. Additionally, we randomly select 300 images from both the Diffusiondb and Pick-a-Pic datasets.

**Model and Training.** We use Stable-Diffusion v-1.5 as the foundation diffusion model for all our experiments. An LMSDiscrete Scheduler is employed with 50 inference steps, and the generated images have a resolution of  $512 \times 512$  pixels. All experiments are conducted using limited computational resources, specifically a single NVIDIA L4 GPU with 22.5GB of memory on Google Colab.

**Reward Models.** We evaluate performance using three distinct reward models, targeting image aesthetics, image-text alignment, and human preference. Specifically, we use the LAION aesthetic predictor V2 (Schuhmann, 2024), the CLIP loss from the multimodal CLIP model (Radford et al., 2021), and the human preference score v2 (Wu et al., 2023). These widely used reward models encompass a wide spectrum of criteria, effectively representing the diverse rewards relevant to text-image alignment tasks.

## 5.2. Benchmarks

We employ the following benchmarks in our evaluation: **Stable diffusion with a raw prompt** (Rombach et al., 2022): We expect IPGO to enhance performance across all datasets and reward models when compared to this baseline. We use two training-based methods: **DRaFT** (Clark et al., 2023) and **DDPO** (Black et al., 2023). DRaFT is functionally identical to AlignProp. Furthermore, we include three training-free methods: **DPO-Diff** (Wang et al., 2024), **Promptist** (Hao et al., 2024), and (following the idea of Mañas et al., 2024) **ChatGPT-4o**. For ChatGPT-4o, we prompt with the instruction: *Improve this sentence to ensure that its stable-diffusion-generated image is {reward-based property}, while remaining concise.* Here, the {reward-based property} is specified as “more aesthetically pleasing,” “more aligned with human preference,” or “more aligned with the original sentence,” depending on the target reward. Detailed qualitative comparisons between the baselines and IPGO are in Appendix A.

## 5.3. Main Results

Due to its flexible gradient-based prompt embedding optimization, we posit that *IPGO more effectively optimizes rewards* compared to the benchmark methods. We perform prompt-wise training for all methods listed in Table 2, where each optimization focuses on a single prompt. To ensure consistency, we establish resource-limited environments across all experiments by limiting the maximum number of training steps to 50 - allowing each full training run on a dataset to complete within one day on a single GPU - and maintaining a similar number of trainable parameters. For DRaFT, we specifically select the DRaFT-1 variant as the baseline, due to its lowest computational cost while anticipating competitive performance (Clark et al., 2023). Details of the hyperparameter settings are provided in Table 3 in Appendix B. We use the best loss value during training to represent each method’s final performance.

Table 1 presents the results of IPGO and the benchmark methods across three datasets, evaluating semantic alignment, aesthetics, and human preference rewards. Note that boldface indicates the highest scores across all models.

When evaluating alignment using CLIP loss, only DRaFT-1 and DDPO are competitive with IPGO. They match IPGO’s performance on the Diffusiondb dataset and for DRaFT-1, on the Pick-a-Pic dataset as well. Additionally, DRaFT outperforms IPGO on the COCO dataset containing images with buildings. In all other scenarios, IPGO surpasses the benchmarks by an average of 3.4%. The comparable results among IPGO, DRaFT-1 and DDPO in three cases are attributable to their use of reward gradients. However, IPGO’s superior performance in all other cases highlights its more efficient use of gradient information. While DPO-Diff also achieves strong results, its discrete search space limits its performance relative to IPGO. Promptist and ChatGPT-4o show minimal improvements, likely due to their limited generalizability to new prompts.

Regarding LAION aesthetics scores, IPGO outperforms all benchmarks across every dataset, achieving an average improvement of 4.4% and often exceeding this margin. Promptist also performs well in improving aesthetics, often ranking second to IPGO. In contrast, ChatGPT 4o demonstrates minimal improvement in optimizing prompts for better aesthetics scores.

For human preference scores, IPGO outperforms all benchmarks across all datasets, achieving an average improvement of 4.2%. Notably, it shows a substantial improvement on the Pick-a-Pic dataset with a 7.7% increase. While most benchmark models struggle to improve the raw prompt in preference scores, IPGO consistently improves performance across all datasets and image categories within the COCO dataset.

	IPGO (%)†	SD v1.5	DRaFT	DDPO	DPO-Diff	Promptist	ChatGPT 4o
<b>Alignment</b>							
<b>COCO</b>							
Person	<b>0.32 (3.2%)</b>	0.26	0.31	0.29	0.29	0.26	0.26
Room	<b>0.29 (3.6%)</b>	0.25	0.28	0.26	0.28	0.24	0.24
Vehicle	<b>0.30 (3.0%)</b>	0.25	0.29	0.28	0.29	0.25	0.25
Natural Scenes	<b>0.29 (3.6%)</b>	0.25	0.28	0.26	0.28	0.23	0.24
Buildings	0.28 (-3.4%)	0.24	<b>0.29</b>	0.27	0.28	0.24	0.24
DiffusionDB	<b>0.32 (0.0%)</b>	0.28	<b>0.32</b>	<b>0.32</b>	0.29	0.28	0.27
Pick-a-Pic	<b>0.31 (0.0%)</b>	0.27	<b>0.31</b>	0.29	0.30	0.26	0.26
<b>Aesthetics</b>							
<b>COCO</b>							
Person	<b>6.22 (4.7%)</b>	5.24	5.78	5.58	4.29	5.94	5.23
Room	<b>5.75 (2.7%)</b>	5.09	5.44	5.37	4.16	5.60	5.24
Vehicle	<b>5.86 (5.4%)</b>	4.96	5.51	5.42	4.02	5.56	5.08
Natural Scenes	<b>5.93 (5.0%)</b>	5.06	5.62	5.51	4.30	5.65	5.16
Buildings	<b>5.80 (2.8%)</b>	5.03	5.43	5.35	4.28	5.64	5.19
DiffusionDB	<b>6.35 (3.9%)</b>	5.50	6.11	5.96	4.44	5.63	5.60
Pick-a-Pic	<b>6.27 (6.3%)</b>	5.32	5.90	5.75	4.36	5.70	5.41
<b>Human Preference</b>							
<b>COCO</b>							
Person	<b>0.29 (3.6%)</b>	0.28	0.28	0.28	0.25	0.27	0.27
Room	<b>0.28 (3.7%)</b>	0.27	0.26	0.27	0.24	0.26	0.27
Vehicle	<b>0.29 (3.6%)</b>	0.28	0.28	0.28	0.25	0.27	0.27
Natural Scenes	<b>0.28 (3.6%)</b>	0.27	0.27	0.27	0.25	0.26	0.27
Buildings	<b>0.28 (3.6%)</b>	0.27	0.27	0.28	0.26	0.26	0.27
DiffusionDB	<b>0.27 (3.8%)</b>	0.26	0.26	0.26	0.25	0.26	0.26
Pick-a-Pic	<b>0.28 (7.7%)</b>	0.26	0.26	0.27	0.25	0.26	0.26

Table 1. Comparison of IPGO’s alignment, aesthetics, and human preference scores against six benchmark models across three datasets and five image categories within the COCO dataset. The percentages reflect how IPGO performs relative to the top-performing benchmark.

Figure 2 qualitatively compares the results generated the raw prompt, IPGO and DRaFT-1 for a random sample of images, evaluated using the HPSv2 reward. Unlike DRaFT-1, which often alters the image layout from that produced by the raw prompt, IPGO tends to modify or add details to the image, while preserving the original layout. Additional image examples are provided in Appendix D.

These findings indicate that IPGO performs very well across datasets and image categories by improving prompts to achieve superior text-image alignment, aesthetics scores, and better human preference scores, particularly effective in improving aesthetics and human preference scores. In 147 scenarios investigated, IPGO has a win rate of 98% over benchmarks, with an average reward improvement of 4.0%.

#### 5.4. Prompt-Batch Training

Similar to DRaFT, IPGO is able to handle prompt batches for training. In this scenario, the learned inserted tokens are shared across all prompts within a batch rather than being unique to each individual prompt, enabling the achievement of more desirable reward properties. Since IPGO modifies the original prompt without altering the diffusion model, we posit that IPGO is more effective in optimizing for higher rewards. To account for the potential effects of prompt heterogeneity within a batch, we conducted experiments using IPGO and Draft-1 with the following setups: (1) 60 prompts from the COCO Person dataset and (2) a mixed batch of 30 prompts from the COCO Person dataset and 30 prompts from the COCO Natural Scenes dataset. We restrict our evaluation to the first 1,000 image generations during

training, use 20 epochs, and employ batch sizes of 4 or 10 (corresponding to 15 or 6 batches per epoch, respectively).

Each row of Figure 4 presents the performances of IPGO and DRaFT-1 across three rewards and two batch sizes on the COCO Person and COCO Mixed datasets. Notably, IPGO achieves the highest improvement in overall Aesthetics among the three rewards, reaching an aesthetic score of 7.0 after 1,000 image generations (with batch size  $B=4$  for COCO Mixed and  $B=10$  COCO Person). In contrast, DRaFT-1 plateaus at an aesthetic score of 5.5 for both datasets. IPGO requires at least 400 image generations to surpass DRaFT. Additionally, a smaller batch size ( $B = 4$ ) is sufficient for the COCO Person dataset, while a larger batch size ( $B = 10$ ) benefits the COCO Mixed dataset.

Regarding Human Preference Scores, IPGO achieves 0.275 on the Mixed dataset compared to 0.270 for DRaFT-1, and 0.282 on the Person dataset versus 0.278 for DRaFT-1. Here, IPGO’s performance remains relatively stable across different numbers of generated images and batch sizes.

However, for CLIP rewards, IPGO struggles to find common tokens that improve overall semantic alignment. Nonetheless, its training curves remain comparable to those of DRaFT-1. This suggests that IPGO is more adept at learning overall stylistic tokens rather than tokens that ensure consistent semantic structures, as finding common tokens that are semantically consistent with all prompts proves more challenging.

Moreover, IPGO demonstrates greater stability than DRaFT-1 with respect to varying batch sizes. In each sub-figure of Figure 4, IPGO’s performance across the two batch sizes is similar, with overlapping fluctuation intervals. In contrast, DRaFT-1 exhibits much more variable performance depending on the batch size. For example, in the CLIP task on Person dataset and the Human Preference task, DRaFT-1’s performance with a batch size of 4 is significantly worse than with a batch size of 10, whereas IPGO’s performance is relatively unaffected by batch size.

In addition, heterogeneity within prompt batches affects both IPGO and DRaFT-1, particularly concerning semantic alignment. Comparing the sub-figures in each row of Figure 4, especially rows 2 and 3, indicates that learning is more efficient when the prompt dataset is more homogeneous (as in the Person dataset). For example, IPGO/DRaFT-1 achieve scores of 0.282/0.276 on the Mixed dataset compared to 0.276/0.270 on the Person dataset. This pattern is expected, as common (prompt) tokens are more effectively extracted from less heterogeneous datasets.

Finally, the learned tokens demonstrate generalizability to unseen prompts, as illustrated in Figure 3. The first row presents images generated from raw prompts, while the second row displays images generated from IPGO prompts

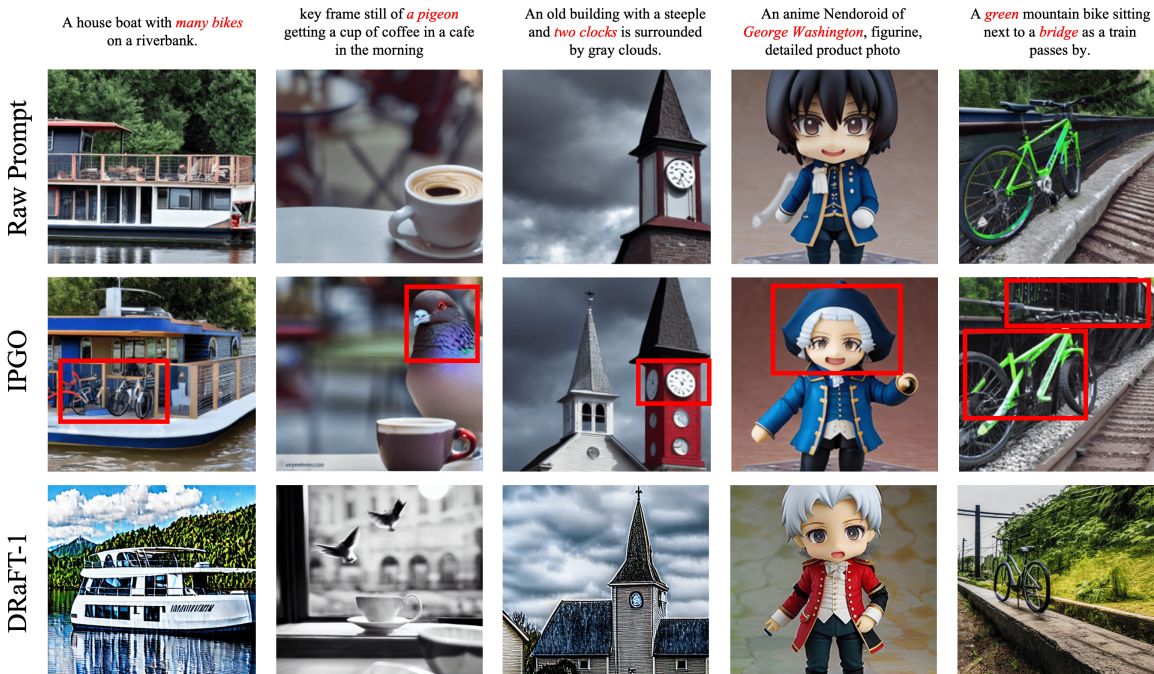


Figure 2. Example images generated by SD v1.5 using the raw prompt (row 1), our IPGO algorithm (row 2) and DRaFT-1 (row 3), evaluated according to the HPSv2 reward. IPGO generates images that are on par with DRaFT-1 and often surpass it in terms of detail. IPGO effectively fine-tunes the original images generated from the raw prompt, enhancing their overall quality.

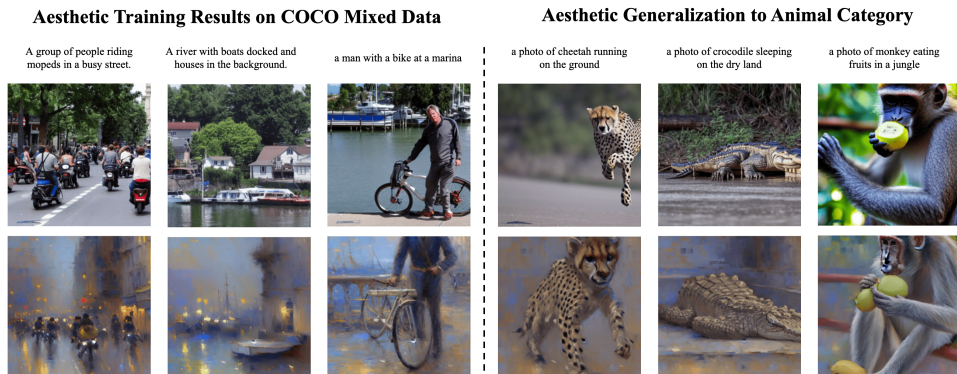


Figure 3. Example images generated by prompt-batch training on the aesthetic reward. The left three columns are the resulting images after training on the COCO Mixed data; the right three columns show images resulting from inserting the trained prefix and suffix in the unseen animal category prompts.

optimized for aesthetic scores. The left three prompts are from the COCO Mixed training data and do not involve any animals, whereas the right three prompts are from the COCO Animals category. Tokens trained on the Mixed data are inserted into the prompt embeddings for the Animals data. The learned water-painting style from aesthetic training is effectively transferred, via the learned prefix and suffix, to the unseen animals prompts. This result underscores the generalizability of IPGO.

Extra results with DiffusionDB and Pick-a-Pic datasets are in Appendix C. Similarly, we find IPGO performs well in

aesthetics and human preference learning, but struggles in CLIP reward relative to DRaFT. Hence, for CLIP alignment, training IPGO with individual prompts is preferred.

### 5.5. Ablation Studies

In this subsection, we provide an in-depth analysis of our design choices, including low rank representation and rotation, as well as hyperparameters:  $N$ , the number of vectors in the orthonormal bases of the prefix and suffix  $E_{pre}$  and  $E_{suf}$ ;  $M_{pre}$  and  $M_{suf}$ , the lengths of the prefix and suffix respectively; and activation of the three constraints: *Value*



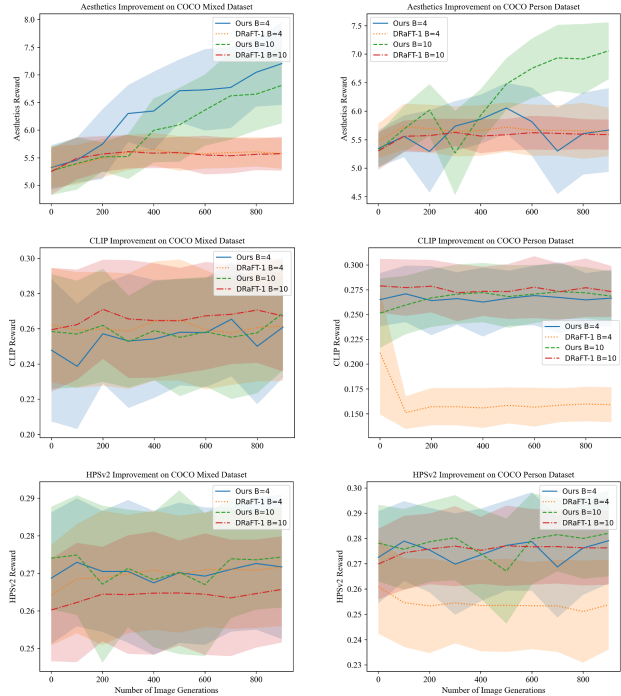


Figure 4. Batch Training results for Aesthetic Reward: Average aesthetic reward score against the number of generated images.

(V), Orthogonality (O) and Conformity (C) constraints.

### Advantages from Low Rank Representation and Rotation

Embedding learning offers an alternative to prefix and suffix learning. We compare the performance of IPGO using this simple embedding scheme against other methods on 60 prompts randomly selected from the COCO dataset. Evaluation is conducted using CLIP rewards averaged across all prompts. In addition, we examine the impact of rotation on these 60 prompts by comparing IPGO’s performances with and without the rotation. The experimental results show that IPGO with rotation achieves a higher average CLIP score of 0.297, slightly better than the 0.295 score obtained without rotation, and significantly outperforms the simple embedding scheme which scores 0.259.

**Benefits of Constraints.** To investigate the impact of the V, O and C constraints on the optimization, we conduct a series of ablation studies. Using the same set of 60 randomly selected prompts as before, we evaluate the average CLIP loss and progressively test various combinations of constraints. First, the *Value* constraint significantly enhances optimization, as evidenced by the substantial improvements in CLIP loss when comparing results without the constraint (0.277) to those with the *Value* constraint alone (0.310). Second, adding the single *Conformity* constraint to the *Value* constraint degrades performance (0.301 v.s. 0.310). However, further imposing the *Orthogonality* constraint sub-

stantially benefits overall optimization (0.322 v.s. 0.310). Therefore, incorporating all three constraints into the search space optimizes the efficiency of our algorithm. Consequently, we employ all three constraints after rotation in our experiments.

**Varying  $N$ .** We investigate the effect of  $N$ , the size of the learnable prompt embeddings, on CLIP reward optimization. Using 30 randomly selected prompts from the COCO dataset, we conduct ablation studies with  $N \in \{5, 10, 20, 30, 40\}$ . We find that the optimal performance occurs at  $N = 30$  (see Figure 6 in Appendix D). Notably, increasing the number of inserted tokens does not necessarily lead to proportional improvements in performance.

**$M_{pre}$  and  $M_{suf}$  based on Raw Prompt Length.** Next, we investigate the optimal prefix and suffix lengths for performance. We experiment with all combinations of prefix and suffix lengths of 0, 5, or 10 tokens, excluding the (0, 0) combination. Using the same 30 randomly selected prompts and evaluating with CLIP reward, we find that the (10, 10) combination yields the highest score of 0.289, while (0, 10) and (10, 0) achieve slightly lower scores of 0.286 each (see Figure 7 in Appendix D for details). These results suggest that performance is improved when the lengths of prefix and suffix are balanced and equal. In addition, we explore the relationship between the raw prompt length and the prefix-suffix length. We use 30 prompts, comprising 10 prompts with only one or two tokens, 10 prompts with approximately 10-15 tokens, and 10 prompts with around 25 tokens. We find no correlation between the raw prompt length and the optimal prefix-suffix length. However, we recommend using fewer inserted tokens for very short prompts to avoid over-parameterization (an illustration is in Appendix D).

## 6. Conclusion

This study presents IPGO, an efficient prompt gradient-based optimization framework to improve diffusion models’ capabilities of generating images with better aesthetics, that are more aligned with the input prompt, and more preferred by humans. We circumvent the discreteness of prompts by inserting prefix and suffix tokens in the prompts’ text encoder embedding. We show, from prompt-wise training, that IPGO improves diffusion model’s reward performance substantially over six benchmarks across three tasks and three datasets, by backpropagating the reward model’s gradients subject to rotation of the prefix and suffix and three constraints: value, orthonormality and conformity. Furthermore, prompt batch learning demonstrates the effectiveness and stability of IPGO, and testifies IPGO’s generalizability to unseen prompts. We believe IPGO has great potential for real-time applications, and hope IPGO can open new possibilities for next-generation image generation.



## Impact Statement

This paper presents work that contributes to the field of Text-to-Image generation models and their applications. In the Machine Learning community, the new method introduced by this paper can broaden the current horizon on fine-tuning diffusion models. In practice, our method can be applied to image related tasks such as automatic real-time image editing.

## References

- Black, K., Janner, M., Du, Y., Kostrikov, I., and Levine, S. Training diffusion models with reinforcement learning. *arXiv preprint arXiv:2305.13301*, 2023.
- Chefer, H., Alaluf, Y., Vinker, Y., Wolf, L., and Cohen-Or, D. Attend-and-excite: Attention-based semantic guidance for text-to-image diffusion models. *ACM Transactions on Graphics (TOG)*, 42(4):1–10, 2023.
- Clark, K., Vicol, P., Swersky, K., and Fleet, D. J. Directly fine-tuning diffusion models on differentiable rewards. *arXiv preprint arXiv:2309.17400*, 2023.
- Dhariwal, P. and Nichol, A. Diffusion models beat gans on image synthesis. *Advances in neural information processing systems*, 34:8780–8794, 2021.
- Esser, P., Kulal, S., Blattmann, A., Entezari, R., Müller, J., Saini, H., Levi, Y., Lorenz, D., Sauer, A., Boesel, F., et al. Scaling rectified flow transformers for high-resolution image synthesis. In *Forty-first International Conference on Machine Learning*, 2024.
- Fan, Y., Watkins, O., Du, Y., Liu, H., Ryu, M., Boutilier, C., Abbeel, P., Ghavamzadeh, M., Lee, K., and Lee, K. Reinforcement learning for fine-tuning text-to-image diffusion models. *Advances in Neural Information Processing Systems*, 36, 2024.
- Frolov, S., Hinz, T., Raue, F., Hees, J., and Dengel, A. Adversarial text-to-image synthesis: A review. *Neural Networks*, 144:187–209, 2021.
- Goodfellow, I., Pouget-Abadie, J., Mirza, M., Xu, B., Warde-Farley, D., Ozair, S., Courville, A., and Bengio, Y. Generative adversarial nets. *Advances in neural information processing systems*, 27, 2014.
- Hao, Y., Chi, Z., Dong, L., and Wei, F. Optimizing prompts for text-to-image generation. *Advances in Neural Information Processing Systems*, 36, 2024.
- Ho, J. and Salimans, T. Classifier-free diffusion guidance. *arXiv preprint arXiv:2207.12598*, 2022.
- Ho, J., Jain, A., and Abbeel, P. Denoising diffusion probabilistic models. *Advances in neural information processing systems*, 33:6840–6851, 2020.
- Hu, E. J., Shen, Y., Wallis, P., Allen-Zhu, Z., Li, Y., Wang, S., Wang, L., and Chen, W. Lora: Low-rank adaptation of large language models. *arXiv preprint arXiv:2106.09685*, 2021.
- Kim, J., Wang, Z., and Qiu, Q. Model-agnostic human preference inversion in diffusion models. *arXiv preprint arXiv:2404.00879*, 2024.
- Kingma, D. P. Auto-encoding variational bayes. *arXiv preprint arXiv:1312.6114*, 2013.
- Kingma, D. P. Adam: A method for stochastic optimization. *arXiv preprint arXiv:1412.6980*, 2014.
- Kirstain, Y., Polyak, A., Singer, U., Matiana, S., Penna, J., and Levy, O. Pick-a-pic: An open dataset of user preferences for text-to-image generation. *Advances in Neural Information Processing Systems*, 36:36652–36663, 2023.
- Li, X., Liu, Y., Isobe, T., Jia, X., Cui, Q., Zhou, D., Li, D., He, Y., Lu, H., Wang, Z., et al. Reneg: Learning negative embedding with reward guidance. *arXiv preprint arXiv:2412.19637*, 2024.
- Li, X. L. and Liang, P. Prefix-tuning: Optimizing continuous prompts for generation. *arXiv preprint arXiv:2101.00190*, 2021.
- Liang, Z., Yuan, Y., Gu, S., Chen, B., Hang, T., Li, J., and Zheng, L. Step-aware preference optimization: Aligning preference with denoising performance at each step. *arXiv preprint arXiv:2406.04314*, 2024.
- Lin, T.-Y., Maire, M., Belongie, S., Hays, J., Perona, P., Ramanan, D., Dollár, P., and Zitnick, C. L. Microsoft coco: Common objects in context. In *Computer Vision—ECCV 2014: 13th European Conference, Zurich, Switzerland, September 6–12, 2014, Proceedings, Part V 13*, pp. 740–755. Springer, 2014.
- Liu, B., Shao, S., Li, B., Bai, L., Xu, Z., Xiong, H., Kwok, J., Helal, S., and Xie, Z. Alignment of diffusion models: Fundamentals, challenges, and future. *arXiv preprint arXiv:2409.07253*, 2024.
- Liu, V. and Chilton, L. B. Design guidelines for prompt engineering text-to-image generative models. In *Proceedings of the 2022 CHI conference on human factors in computing systems*, pp. 1–23, 2022.
- Mañas, O., Astolfi, P., Hall, M., Ross, C., Urbanek, J., Williams, A., Agrawal, A., Romero-Soriano, A., and Drozdal, M. Improving text-to-image consistency

- via automatic prompt optimization. *arXiv preprint arXiv:2403.17804*, 2024.
- Nichol, A., Dhariwal, P., Ramesh, A., Shyam, P., Mishkin, P., McGrew, B., Sutskever, I., and Chen, M. Glide: Towards photorealistic image generation and editing with text-guided diffusion models. *arXiv preprint arXiv:2112.10741*, 2021.
- Oppenlaender, J. A taxonomy of prompt modifiers for text-to-image generation. *Behaviour & Information Technology*, pp. 1–14, 2023.
- Peebles, W. and Xie, S. Scalable diffusion models with transformers. In *Proceedings of the IEEE/CVF International Conference on Computer Vision*, pp. 4195–4205, 2023.
- Podell, D., English, Z., Lacey, K., Blattmann, A., Dockhorn, T., Müller, J., Penna, J., and Rombach, R. Sdxl: Improving latent diffusion models for high-resolution image synthesis. *arXiv preprint arXiv:2307.01952*, 2023.
- Prabhudesai, M., Goyal, A., Pathak, D., and Fragkiadaki, K. Aligning text-to-image diffusion models with reward backpropagation. *arXiv preprint arXiv:2310.03739*, 2023.
- Radford, A., Kim, J. W., Hallacy, C., Ramesh, A., Goh, G., Agarwal, S., Sastry, G., Askell, A., Mishkin, P., Clark, J., et al. Learning transferable visual models from natural language supervision. In *International conference on machine learning*, pp. 8748–8763. PMLR, 2021.
- Ramesh, A., Dhariwal, P., Nichol, A., Chu, C., and Chen, M. Hierarchical text-conditional image generation with clip latents. *arXiv preprint arXiv:2204.06125*, 1(2):3, 2022.
- Rombach, R., Blattmann, A., Lorenz, D., Esser, P., and Ommer, B. High-resolution image synthesis with latent diffusion models. In *Proceedings of the IEEE/CVF conference on computer vision and pattern recognition*, pp. 10684–10695, 2022.
- Saharia, C., Chan, W., Saxena, S., Li, L., Whang, J., Denton, E. L., Ghasemipour, K., Gontijo Lopes, R., Karagol Ayan, B., Salimans, T., et al. Photorealistic text-to-image diffusion models with deep language understanding. *Advances in neural information processing systems*, 35: 36479–36494, 2022.
- Samuel, D., Ben-Ari, R., Raviv, S., Darshan, N., and Chechik, G. Generating images of rare concepts using pre-trained diffusion models. In *Proceedings of the AAAI Conference on Artificial Intelligence*, volume 38, pp. 4695–4703, 2024.
- Schuhmann, C. Laion aesthetic predictor. <https://laion.ai/blog/laion-aesthetics/>, 2024.
- Sohl-Dickstein, J., Weiss, E., Maheswaranathan, N., and Ganguli, S. Deep unsupervised learning using nonequilibrium thermodynamics. In *International conference on machine learning*, pp. 2256–2265. PMLR, 2015.
- Song, Y. and Ermon, S. Generative modeling by estimating gradients of the data distribution. *Advances in neural information processing systems*, 32, 2019.
- Su, J., Ahmed, M., Lu, Y., Pan, S., Bo, W., and Liu, Y. Roformer: Enhanced transformer with rotary position embedding. *Neurocomputing*, 568:127063, 2024.
- Wallace, B., Dang, M., Rafailov, R., Zhou, L., Lou, A., Purushwalkam, S., Ermon, S., Xiong, C., Joty, S., and Naik, N. Diffusion model alignment using direct preference optimization. In *Proceedings of the IEEE/CVF Conference on Computer Vision and Pattern Recognition*, pp. 8228–8238, 2024.
- Wang, R., Liu, T., Hsieh, C.-J., and Gong, B. On discrete prompt optimization for diffusion models. *arXiv preprint arXiv:2407.01606*, 2024.
- Wang, Y., Shen, S., and Lim, B. Y. Reprompt: Automatic prompt editing to refine ai-generative art towards precise expressions. In *Proceedings of the 2023 CHI conference on human factors in computing systems*, pp. 1–29, 2023.
- Wang, Z. J., Montoya, E., Munechika, D., Yang, H., Hoover, B., and Chau, D. H. Diffusiondb: A large-scale prompt gallery dataset for text-to-image generative models. *arXiv preprint arXiv:2210.14896*, 2022.
- Wen, Y., Jain, N., Kirchenbauer, J., Goldblum, M., Geiping, J., and Goldstein, T. Hard prompts made easy: Gradient-based discrete optimization for prompt tuning and discovery. *Advances in Neural Information Processing Systems*, 36, 2024.
- Wu, X., Hao, Y., Sun, K., Chen, Y., Zhu, F., Zhao, R., and Li, H. Human preference score v2: A solid benchmark for evaluating human preferences of text-to-image synthesis. *arXiv preprint arXiv:2306.09341*, 2023.
- Wu, Y., Cao, X., Li, K., Chen, Z., Wang, H., Meng, L., and Huang, Z. Towards better text-to-image generation alignment via attention modulation. *arXiv preprint arXiv:2404.13899*, 2024.
- Xu, J., Liu, X., Wu, Y., Tong, Y., Li, Q., Ding, M., Tang, J., and Dong, Y. Imagereward: Learning and evaluating human preferences for text-to-image generation. *Advances in Neural Information Processing Systems*, 36, 2024.

- Yang, K., Tao, J., Lyu, J., Ge, C., Chen, J., Shen, W., Zhu, X., and Li, X. Using human feedback to fine-tune diffusion models without any reward model. In *Proceedings of the IEEE/CVF Conference on Computer Vision and Pattern Recognition*, pp. 8941–8951, 2024a.
- Yang, L., Yu, Z., Meng, C., Xu, M., Ermon, S., and Bin, C. Mastering text-to-image diffusion: Recaptioning, planning, and generating with multimodal llms. In *Forty-first International Conference on Machine Learning*, 2024b.
- Żelaszczyk, M. and Mańdziuk, J. Text-to-image cross-modal generation: A systematic review. *arXiv preprint arXiv:2401.11631*, 2024.
- Zhang, C., Zhang, C., Zhang, M., and Kweon, I. S. Text-to-image diffusion models in generative ai: A survey. *arXiv preprint arXiv:2303.07909*, 2023.
- Zheng, G., Zhou, X., Li, X., Qi, Z., Shan, Y., and Li, X. Layoutdiffusion: Controllable diffusion model for layout-to-image generation. In *Proceedings of the IEEE/CVF Conference on Computer Vision and Pattern Recognition*, pp. 22490–22499, 2023.

## A. Qualitative Comparisons among Methods

Table 2 qualitatively compares our IPGO algorithm with the benchmarking algorithms outlined in Section 5.2. As can be seen from the table, IPGO is the only method that leverages reward gradient computation, supports prompt modification and batch training, and maintains low computational search costs.

<i>Algorithms</i>	<i>Reward Gradient</i>	<i>Prompt Modification</i>	<i>Batch Training</i>	<i>Search Space Cost</i>
Promptist	✗	✓	✓	High (SFT required)
DPO-Diff	✓	✓	✗	High (External LLM required)
DRaFT	✓	✗	✓	Low
DDPO	✗	✗	✓	High (Many samples required)
ChatGPT-4o	✗	✓	✗	Low
IPGO (ours)	✓	✓	✓	Low

Table 2. A qualitative comparison between IPGO and all benchmarks, focusing on four key aspects: the ability to compute reward gradients, support for prompt modification, compatibility with batch training, and the computational cost of searching the prompt space.

## B. Implementation Details

This section provides details on IPGO’s implementation and training.

**Image Generation** We use LMSD scheduler with 50 sampling steps under a guidance weight of 7.5, constant throughout training and testing cases. We found similar performances with other sampling strategies, such as PNLM and DDIM.

**Optimization** We train IPGO using Adam (Kingma, 2014) optimizer without a weight decay. For prompt-wise training, we start with a learning rate of  $1e - 3$  and reduce it by a factor of 0.9 every 10 epochs, continuing this schedule for a total of 50 epochs. In contrast, for prompt-batch training, we maintain a constant learning rate of  $1e - 3$  over 20 epochs.

**Hyperparameters** We set the hyperparameters of IPGO and DRaFT-1 to ensure that the total number of trainable parameters is comparable. IPGO includes the hyperparameters  $N$ ,  $M_{pre}$  and  $M_{suf}$ , while DRaFT-1 has a low rank for the LoRA parameters in the UNet. For DDPO, we simply use the default configurations. Detailed hyperparameter settings for IPGO, DRaFT-1 and DDPO are provided in Table 3.

<i>Methods</i>	<i>Hyperparameter</i>	<i>Value</i>
IPGO	$N$	30
	$M_{pre}$	10
	$M_{suf}$	10
Total #parameters		468,376
DRaFT-1	LoRA rank	6
Total #parameters		597,888
DDPO	Default DDPOTrainer Configuration	
Total #parameters		860,318,148

Table 3. Hyperparameter settings for IPGO, DRaFT-1 and DDPO

**IPGO’s Constraints** IPGO has three constraints: Orthogonality, Value and Conformity constraints. We enforce the orthogonality constraint with `orthogonal()` module in Pytorch. For the value constraint, we clamp the parameters to satisfy the constraint after each update. Finally, for simplicity, we use a soft conformity constraint in the optimization instead



of a hard one. We add a conformity penalty to the objective, the negative image reward. Define the conformity penalty by

$$p_{conf} = \left\| \frac{1}{J} \sum_{j=1}^J T_j - \frac{1}{K} \sum_{k=1}^K f(C)_k \right\|_2^2, \quad (11)$$

where  $T$  and  $f(C)$  are the modified prompt embeddings and original prompt embeddings, respectively. Then the optimization objective becomes:

$$\mathcal{L} = -\mathcal{R}(x, C) + \gamma p_{conf}, \quad (12)$$

where  $\mathcal{R}(x, C)$  is one of the Aesthetic, CLIP and HPSv2 reward scores as a function of the image  $x$  and prompt  $C$  (or their weighted combination), and  $\gamma$  is the conformity coefficient. Our experiments set  $\gamma = 1e - 3$ .

### The Full Algorithm of IPGO

---

#### Algorithm 1 IPGO

**Input:** Raw prompt  $C$ , prefix  $T_{pre}$ , suffix  $T_{suf}$ , text encoder  $f(\cdot)$ , diffusion model  $SD(\cdot)$ , image reward model  $R(\cdot)$ , conformity penalty coefficient  $\gamma$ , learning rate  $\eta$ , number of epochs  $P$   
**Output:** Optimal prefix  $T_{pre}^*$  and suffix  $T_{suf}^*$ .  
**for**  $i = 0$  **to**  $P$  **do**  
    Original prompt embedding:  $T_0 = f(C)$ .  
    Insert prefix and suffix:  $T = [T_{pre}, T_0, T_{suf}]$ .  
    Sample image:  $x = SD(T)$ .  
    Compute reward:  $r = \mathcal{R}(x, C)$ .  
    Compute objective:  $\mathcal{L} = -r + \gamma p_{conf}$ .  
    Compute (prefix,suffix) gradient:  $g = \nabla_{(T_{pre}, T_{suf})} \mathcal{L}$ .  
    Update prefix and suffix:  $(T_{pre}, T_{suf}) \leftarrow (T_{pre}, T_{suf}) - \eta g$ .  
    Enforce Orthogonality and Value constraints.  
**end for**  
Return  $T_{pre}^*$  and  $T_{suf}^*$ .

---

### C. Additional Results

**Extra Prompt-batch Results** We present additional experimental results for prompt-batch training on the DiffusionDB and Pick-a-Pic datasets. For each dataset, we randomly select 60 prompts and conduct tests only with a batch size of  $B = 10$ . Like in Section 5.4, we compare the performance of IPGO with that of the strongest benchmark model, DRaFT-1. The choice of  $B = 10$  is motivated by DRaFT’s optimal performance on the COCO datasets at this batch size, as illustrated in Figure 4). Our results thus present a lower bound on the potential performance gains of IPGO.

Figure 5 presents the results, with the first row corresponding to the DiffusionDB dataset and the second row to the Pick-a-Pic dataset. First, similar to the findings from prompt-batch training on the COCO dataset, IPGO achieves higher aesthetics scores, with these scores improving rapidly compared to the other two reward scores. These improvements begin to materialize after approximately 400-500 image generations. Second, IPGO significantly outperforms DRaFT-1 in terms of HPSv2 scores. DRaFT-1 appears to struggle with improving prompts to achieve better human preference scores, indicating that prompt-level optimization is more robust than fine-tuning the UNet in the stable diffusion model. Third, IPGO faces challenges in improving CLIP alignment scores for the Pick-a-Pic dataset. The prompts in this dataset are complex and contain extensive stylistic and other information. IPGO finds it difficult to improve those complex, lengthy prompts during batch training for alignment, likely due to the difficulty in identifying common pre- and suffix tokens that help better align the syntax of the prompts with the images. Consequently, while IPGO does not perform as well in batch training for complex prompts in terms of CLIP alignment, it still surpasses DRaFT and other benchmarks in individual training. Therefore, we recommend training IPGO on individual prompts for alignment problems.

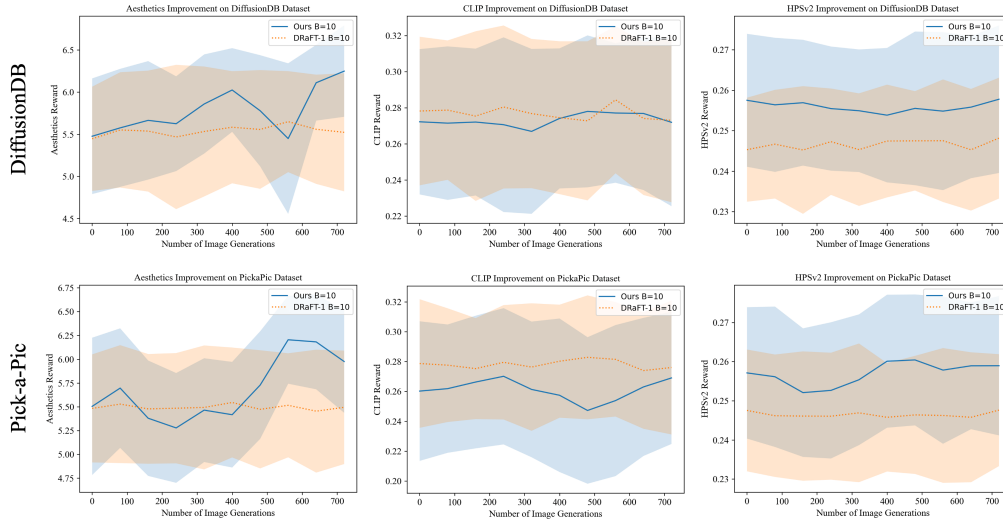


Figure 5. Additional experiments for prompt-batch training on DiffusionDB and Pick-a-Pic datasets. We observe similar patterns as for the COCO dataset.

## D. Details of Ablation Studies

**Varying  $N$**  Figure 6 illustrates the average CLIP scores across varying sizes of orthonormal basis. We find that an optimal basis size of  $N = 30$  exists, although this is not immediately apparent. This finding aligns with expectations, as it reflects the inherent trade-off between the size of the search space and performance: a small search space undermines the optimization freedom, while an excessively large search space increases the optimization difficulty as well.

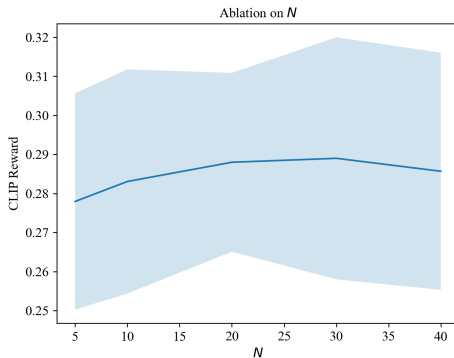


Figure 6. Experiment on  $N$ , the size of the orthonormal basis. There exists an optimal value at  $N = 30$

**$M_{pre}$  and  $M_{suf}$  based on Raw Prompt Length** Figure 7 presents a table that contains average CLIP scores of all possible combinations of  $M_{pre}$  and  $M_{suf} \in \{0, 5, 10\}$  in our experiment. We observe that a balance of the prefix and suffix lengths tends to give a better performance. For combinations that have 5 (or 10) as the maximum length, (5, 5) (or (10, 10)) always yields the best performance, with the latter being the highest.

Next, we test the relationship between the length of the raw prompt and the lengths of prefix and suffix. We choose 30 prompts among which the first 10 prompts are simple prompts, such as “Man”, “Woman” and “Student”, the second 10 prompts are medium-complexity prompts, selected from the COCO dataset, and the last 10 prompts are even more complex versions of the second 10 prompts by inquiring ChatGPT-4o with “Could you make the following 10 prompts more complex:.” For example, the complex version of “A person walking in the rain while holding an umbrella.” is “A middle-aged person in a long, tattered trench coat walks down a cobblestone street, their brightly colored umbrella catching

		$M_{pre}$		
		0	5	10
$M_{suf}$	0	/	0.281	0.286
	5	0.284	0.284	0.286
	10	0.286	0.284	<b>0.289</b>

Figure 7. Experiments on  $M_{pre}$  and  $M_{suf}$ . The table shows that a balanced prefix and suffix length at 10 yields the best performance.

the dim glow of streetlights as rain cascades around them.” We make sure that the complex sentences do not exceed the limit of 77 tokens. We optimize each prompt with  $M_{pre} = M_{suf} = M \in \{2, 10, 15\}$  with respect to the CLIP reward. We use the distribution of the number of prompts that respectively have  $M = 2, 10, 15$  as their best prefix and suffix lengths in each prompt group as the evaluation metric. For simplicity, we denote this distribution as  $D_M(2, 10, 15)$ .

We do not observe a significant correlation between the prompt length and the prefix and suffix lengths. The simple prompt group has  $D_M(2, 10, 15) = (30\%, 50\%, 20\%)$ ; the medium-complex prompt group has  $D_M(2, 10, 15) = (50\%, 20\%, 30\%)$ ; and the complex prompt group has  $D_M(2, 10, 15) = (20\%, 40\%, 40\%)$ . We observe a weak positive relationship of  $M$  with the raw prompt length at best.

**Overparameterization** IPGO faces the risk of overparameterization when the lengths of the prefix and suffix significantly exceed that of the raw prompt. For example, Figure 8 illustrates this issue with an extreme example, showcasing the evolution of images generated during the optimization of the simple prompt “cat” with very long  $M_{pre} = M_{suf} = 30$  for aesthetics improvement. In the first several steps, IPGO produces images that display a cat, but at later steps, the object in the image changes to a person, and at even later steps the specific person also changes. Apparently, if the prefix and suffix are too long, then in spite of the conformity constraint, optimization of the inserted tokens overwhelms the semantic structure of the image and harms alignment of the image with the *original* prompt. Therefore, we recommend using shorter prefix and suffix lengths for shorter prompts.

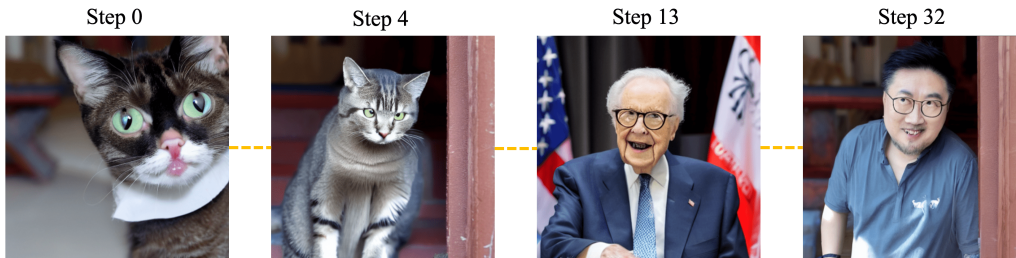


Figure 8. Images generated during IPGO’s optimization on the prompt “Cat” with  $M_{pre} = M_{suf} = 30$  for aesthetics. Because of overparameterization the images that are produced show poor alignment with the *original* prompt.



## E. Additional Image Examples

### E.1. Additional Comparisons with DRaFT-1

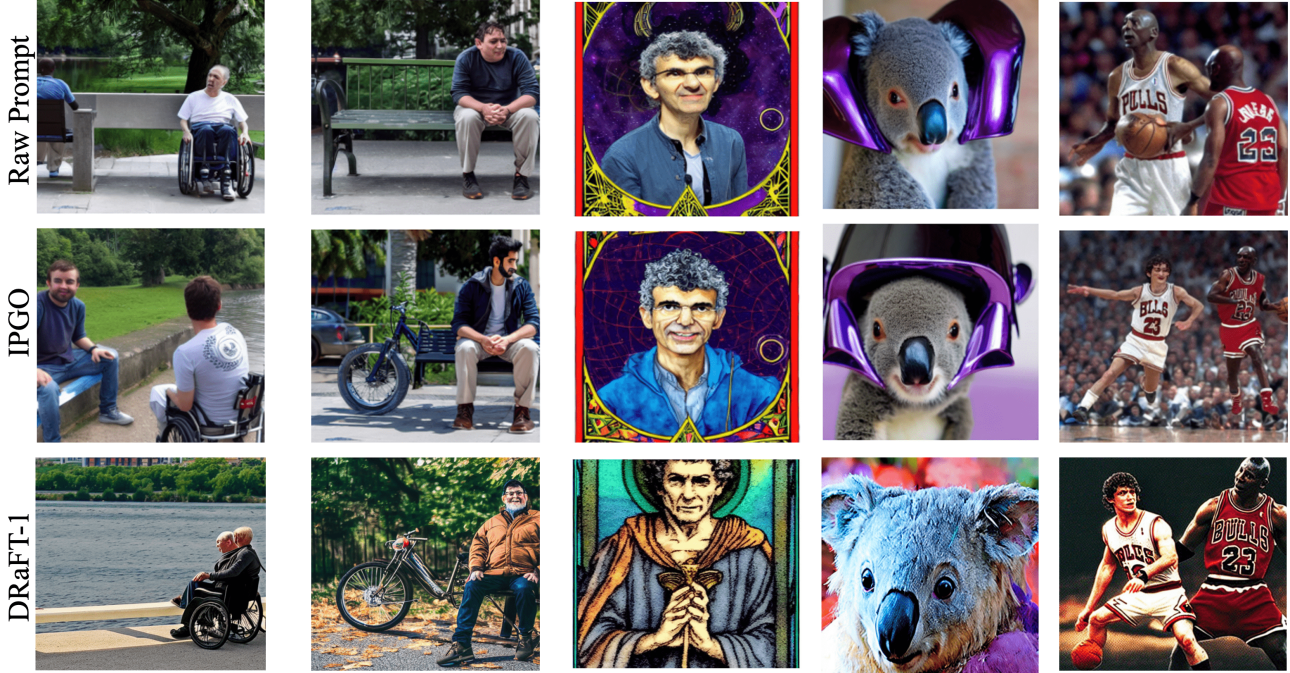
*A man in a wheelchair and another sitting on a bench that is overlooking the water.*

*A man is sitting on a bench next to a bike.*

*Yoshua Bengio on the Tarot Hermit card. Illustration by Pamela Colman Smith*

*a koala wearing a purple chrome darth vader helmet on a koala*

*frodo baggins blocking michael jordan, nba*



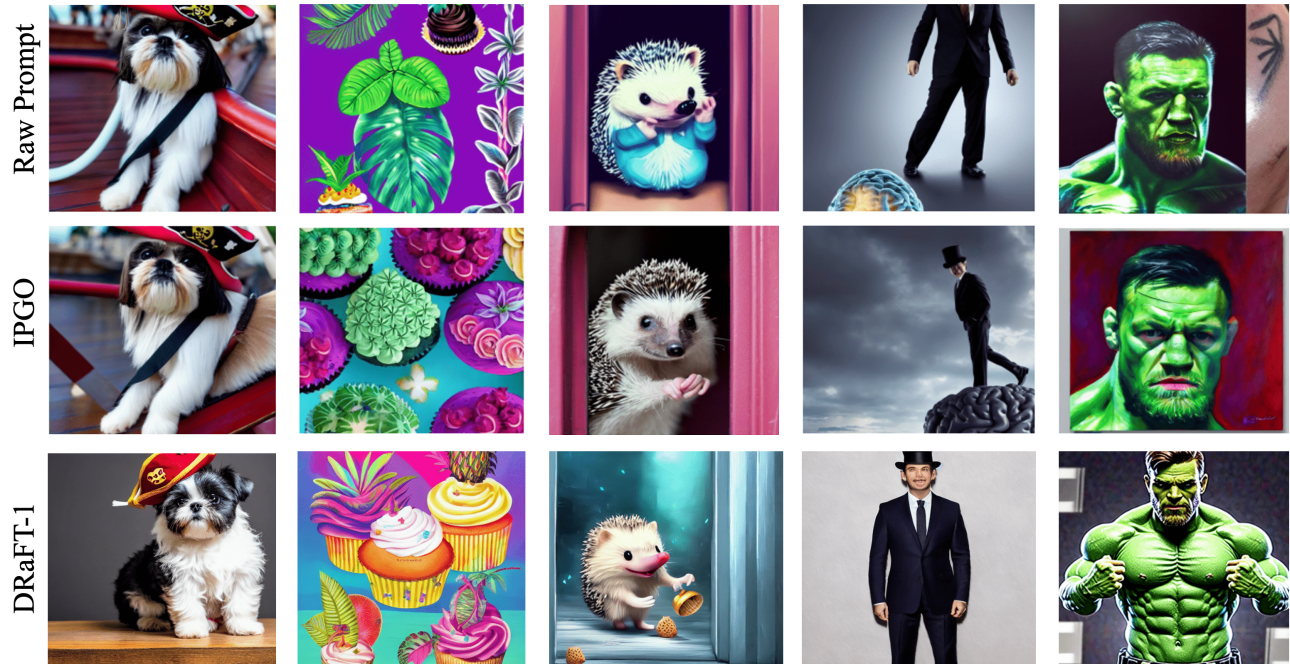
*a shih tzu on a pirate ship, wearing pirate hat, canon eos r, 3..., in - frame*

*a painting of tropical plants and inverted cupcakes by lisa frank, behance, airbrush art, digital painting*

*cute adorable hedgehog opening the door, waving, smiling, cute, hedgehog, by cyril rolando*




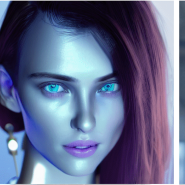
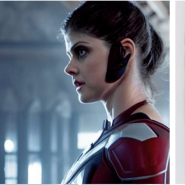

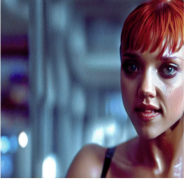
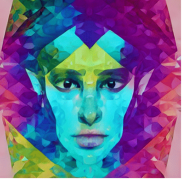

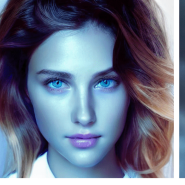





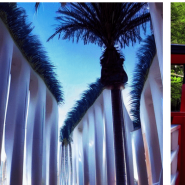









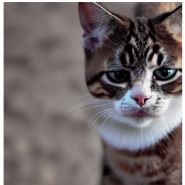

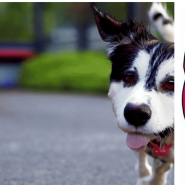
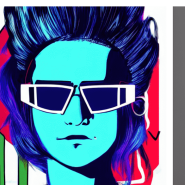

*Photograph of a man in a suit and bowler hat standing on the surface of a giant brain. Realistic.*

*connor mcgregor dressed as hulk, 8 k, trending on artstation, smooth, ..., annie leibowitz*





E.2. Others

	movie still from the fifth element, body portrait of a young woman jessica alba cyborg ...	colorful graffiti, shards, illustration, highly detailed, simple, no jagged lines, smooth, antistation, centered artwork by shepard fairey of centered portrait of an elfen	a highly detailed beautiful portrait of hamster playing poker, by gregory manches, james gurney, james jean	These 3D portraits are unbelievably realistic, unreal engine 5 RTX raytracing nvidia hairworks render of portrait of the most beautiful girl with blue eyes.	movie film still of Alexandra Daddario as a female Colossus in a new X-Men movie, cinematic	caricature angry old man in chair inside a dark house, painting by by ralph grady james, jean christian biville
Raw Prompt						
IPGO						
	photo of a group of female doctors, working in a hospital	a pov shot, color cinema film still of saul goodman & kate perry in blade runner 2 0 4 9, cinematic lighting at night.	70 mm portrait, furry rocket the raccoon sitting in the cockpit of the millennium falcon, ... photorealism!!	futuristic utopian paradise, canals, bridges, white marble temples, palm trees, ... cinematic lighting,, pinterest	a shinto shrine path atop a mountain, spring, cherry trees, beautiful nature, distant shot, random angle	backlit levitating geert wilders raising both his arms amid a crowd, aesthetic
Raw Prompt						
IPGO						
	a highly detailed symmetrical painting of a female sorcerer with piercing eyes in a dungeon, ... glenn fabry	RAW photo of a cute cat as a cowboy standing in a desert, bokeh	Photo of a blonde 18yo cyborg girl, intricate white cyberpunk respirator and armor	genere una imagen de un perro pequeño feliz , jugando y corriendo por el parque	a drawing of a girl with bright blue hair wearing sunglasses, cyberpunk art ..., pop art	portrait of a Young woman with short blonde hair wearing glasses and freckles around her nose
Raw Prompt						
IPGO	